Jurnal Teknologi, 38(F) Jun. 2003: 65–86

ON THE NUMERICAL SIMULATION OF RAPID PRESSURE SWING ADSORPTION FOR AIR SEPARATION

THOMAS S.Y. CHOONG[1], WILLIAM R. PATERSON[2] & DAVID M. SCOTT[3]

Abstract. The physically consistent rapid pressure swing adsorption (RPSA) models developed by Choong [5] are solved numerically by spatially discretisating the partial differential equations (PDEs) to a system of ordinary differential equations (ODEs), which are then integrated over time. Two spatial discretisation methods are considered, namely the methods of orthogonal collocation (OC) and orthogonal collocation on finite elements (OCFE). The RPSA simulation programs are validated by simplifying the process models to compare the numerical results with similarity solutions obtained by Scott (1991) for air pressurisation and depressurisation into a semi-infinite adsorbing bed. The error in conservation of mass is computed as a guide to the numerical accuracy of the calculations. To ensure good accuracy in the calculation of conservation of mass, all the time integrals were transformed into ODEs. With the transformation, the accuracy of the numerical calculations depends only on the spatial discretisation and the tolerance used in the ODE integration algorithm. The effect of the spatial discretisation and the value of TOL on the accuracy of the numerical results and the computer processing time is studied. A rule of thumb to estimate the value of TOL is proposed. The method of OC is found to give accuracy comparable to that of the method of OCFE, albeit requiring more computing time. The method of OC is considered sufficient for the purpose of our future work, such as to develop novel algorithm features for cyclic processes.

Key words: Rapid pressure swing adsorption, modelling, numerical simulation, air separation

Abstrak. Model penjerapan buai tekanan deras yang kosisten (RPSA) secara fizikal telah dibangunkan oleh Choong (2000). Model ini boleh diselesaikan secara berangka dengan menjelmakan persamaan kebezaan separa kepada sistem persamaan kebezaan biasa (ODE). Seterusnya, sistem ODE dikamirkan terhadap masa. Dua kaedah pendiskretan ruang dipertimbangkan, iaitu kaedah penempatan bersama ortogon (OC) dan penempatan bersama ortogon terhadap unsur terhingga (OCFE). Program penyelakuan RPSA disahkan menggunakan model proses supaya dapat dibandingkan keputusan berangka dengan penyelesaian keserupaan yang diperoleh oleh Scott (1991), bagi penekanan dan penyahtekanan udara terhadap lapisan penjerapan separuh tak terhingga. Ralat keabadian jisim digunakan sebagai pengukur kepada kejituan pengiraan berangka. Bagi menjamin hasil pengiraan keabadian jisim yang jitu, semua kamiran masa dijelmakan kepada ODE. Dengan jelmaan ini, kejituan pengiraan berangka hanya bergantung kepada pendiskretan ruang dan had terima yang digunakan dalam algoritma pengamiran ODE. Kesan pendiskretan ruang dan nilai had terima yang digunakan dalam penyelesaian ODE (TOL) terhadap ketepatan keputusan berangka dan masa pemprosesan komputer dikaji. Suatu sekaitan untuk menganggar TOL dicadangkan. Walaupun kaedah OC memerlukan masa pengkomputeran yang lebih panjang, tetapi keputusan yang dihasilkan

[1] Department of Chemical and Environmental Engineering, Universiti Putra Malaysia, 43400 Serdang, Malaysia. Fax: (603)-86567099; E-mail: tsyc2@eng.upm.edu.my

[2&3] Department of Chemical Engineering, University of Cambridge, Pembroke Street, Cambridge, CB2 3RA, U.K.

lebih jitu berbanding kaedah OCFE. Kaedah OC sesuai digunakan untuk projek masa depan kami seperti membangunakan ciri algoritma bagi proses berkitar.

Kata kunci: Penjerapan buai tekanan deras, pemodelan, penyelakuan berangka, pemisahan udara

1.0 INTRODUCTION

This work is concerned with the separation of oxygen from air using a unique version of Pressure Swing Adsorption (PSA), rapid pressure swing adsorption (RPSA), with zeolite 5A as adsorbent. Since nitrogen has a higher tendency to adsorb on zeolite 5A than oxygen, nitrogen is preferentially adsorbed on the adsorbent, giving oxygen-enriched air in the bulk gas phase. Oxygen product purity up to 90% can be produced using RPSA [1].

For a complex process such as RPSA, insights into the behaviour of the system might be difficult to gain through experience and intuition alone. Numerical simulation is thus a useful tool for an engineer to study the behaviour of an actual RPSA process. Simulation also provides a convenient, inexpensive, and safe method of gaining insights into the process.

Hassan *et al*. [2] demonstrated that for cyclic adsorption problems, the method of orthogonal collocation (OC) is substantially more efficient than finite difference methods. Alpay [3] compared a number of numerical methods in solving RPSA models such as the methods of OC, Orthogonal Collocation of Finite Elements, double orthogonal collocation on finite elements and cell-in-series. He concluded that the method of (OCFE) is the most efficient method in terms of computing time.

However, as established by Choong *et al*. [4], the model formation employed by Alpay [3] did not conserve mass. Therefore, the status of his results is unclear. Futhermore, the subroutine used by Alpay [3] to solve the non-linear algebraic equations in the OCFE was not appropriate. The NAG FORTRAN library subroutine FO4EAF used by Alpay [3] is only suitable for solving linear algebraic equations, but not for non-linear algebraic equations as encountered in this work.

The purpose of this paper is to re-examine the conclusion of Alpay [3]. In addition, a study was conducted on the effect of spatial discretisation and the value of TOL on the accuracy of the numerical results and the computer processing time (CPU) required in the calculations. A physically consistent model formulation recommended by Choong *et al.* [4] was used. In this work, computer programs written in FORTRAN 77 were developed for both the instantaneous (ILE) model and the linear driving force (LDF) model using OC. An ILE model using the OCFE method using equally sized elements with polynomials of the same order in each element [3,5,6] was also considered. The computer programs were validated:

(a) using a case of heat conduction for which analytical solutions were available, and
(b) by simplifying the process models so that the numerical results could be compared with similarity solutions obtained by Scott [7] for air pressurisation and depressurisation in a semi-infinite adsorbing bed.

2.0 PROCESS DESCRIPTION

The RPSA was originally developed by Turnock and Kadlec [8]. It employs only a single packed bed, with very short cycle times (in the order of seconds) and small particle size (typically 200–700 μm in diameter). Compared with conventional PSA systems, it has the advantage of process simplicity and higher production rate at equal purity and recovery [1].

A basic RPSA cycle consists of two steps: pressurisation and depressurisation, as illustrated in Figure 1. During pressurisation, air is fed to the column through a three-way valve. Pressure increases rapidly at the feed end of the column. As feed air flows down the column, nitrogen is preferentially adsorbed on the zeolite 5A adsorbent, resulting in an oxygen-enriched gas phase.

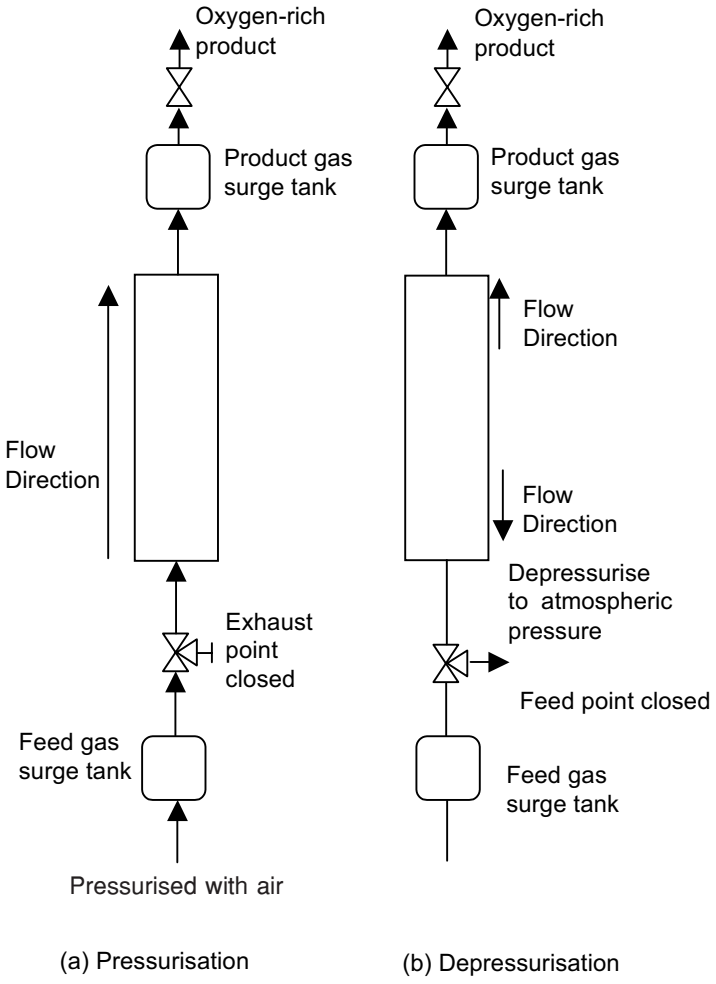

Figure 1 Basic steps in RPSA [8]

In the depressurisation step, the feed valve is closed and the exhaust valve at the feed end is opened to atmospheric pressure, resulting in a rapid pressure drop at the feed end of the column, followed by desorption of the adsorbed nitrogen. The gas leaving the exhaust port is enriched with nitrogen. As there is a pressure maximum in the bed during depressurisation, a pressure gradient is always maintained between this maximum and the product end of the bed, which results in a continuous product stream throughout the cycle. Since the feed and product flowrates are unsteady, surge tanks are needed in some applications to smooth the flows. A delay step, placed between the pressurisation and depressurisation steps, is sometimes used to allow the pressure wave to penetrate further into the bed.

In this work, a cycle always starts at the start of pressurisation and is viewed as complete at the instant of finishing the depressurisation step. The delay step is not included and equal pressurisation and depressurisation times are used. The dynamics of the feed and product surge tanks are not considered. The resistance in gas pipe lines and dead volumes that might exist upstream and downstream of the packed bed are assumed to be negligible.

3.0 MATHEMATICAL MODELS

Two RPSA models were used, namely the instantaneous local equilibrium (ILE) model and the linear driving force (LDF) model. A rich, binary gas mixture consisting of oxygen (component A) and nitrogen (component B) was considered. The subscript i refer to component i, where $i = A, B$. The assumptions made:

(1) The ideal gas law is obeyed.
(2) The process is assumed to be isothermal.
(3) The bed is packed uniformly with spherical particles.
(4) The flow pattern is described by the axially dispersed plug flow (ADPF) model with a constant axial dispersion coefficient.
(5) Gas flow is described by Darcy's Law.
(6) Adsorption isotherms for both oxygen and nitrogen are given by Henry's Law.
(7) The radial temperature and concentration gradients are negligible.
(8) A step change of pressure at the feed end occurs for both pressurisation and depressurisation steps.
(9) The product delivery rate is constant with time.
(10) The packed bed is initially in equilibrium with atmospheric air.

The RPSA models were formulated to conserve mass, such as by writing the Fickian flux models that describe the axial dispersion and the boundary conditions (BCs) in terms of mole fractions [4].

The gas flow through a packed bed is described by Darcy's law and as suggested by MacDonald *et al.* [9].

$$\frac{dP}{dz} = -J_v u = -180\frac{\mu(1-\varepsilon_b)^2}{d_p^2\varepsilon_b^3}u \tag{1}$$

3.1 Instantaneous Local Equilibrium (ILE) Model

The simplest mathematical model for PSA processes assumes that all the mass transfer resistances, including those outside and inside the adsorbent particles, are negligible. In RPSA, the ILE assumption is valid at large cycle times and for small particle sizes, but is not justified at small cycle times and for large particle sizes [3]. However, the ILE model requires much less computing time than mass transfer models, hence it is used as a preliminary tool to test the numerical methods for solving the PDEs.

For the ILE model, the gas phase in the pores is assumed to have the same concentration as in the bulk gas phase and the adsorbed phase is in equilibrium with the bulk gas phase.

The governing equations are:

$$\frac{\partial y_A}{\partial t} = \frac{-1}{(\varepsilon_t + \rho_b H_A)P}\left\{\frac{\partial(uPy_A)}{\partial z} - D\frac{\partial}{\partial z}\left(P\frac{\partial y_A}{\partial z}\right)\right\} - \frac{y_A}{P}\frac{\partial P}{\partial t} \tag{2}$$

and

$$\frac{\partial P}{\partial t} = \frac{-1}{(\varepsilon_t + \rho_b H_B)}\left\{\frac{\partial(uP)}{\partial z} - \frac{\rho_b(H_A - H_B)}{\varepsilon_t + \rho_b H_A}\left\{\frac{\partial(uPy_A)}{\partial z} - D\frac{\partial}{\partial z}\left(P\frac{\partial y_A}{\partial z}\right)\right\}\right\} \tag{3}$$

3.2 Linear Driving Force Model

As high porosity is desirable for commercial adsorbents, the overall adsorption rate is usually limited by diffusion into the adsorbent particles. A complete description of the column dynamics in an RPSA process requires the solution of both bed and particle mass balances. This situation could be simplified by replacing the diffusion equation in the particle with a space-independent approximation for the rate of adsorption, $d\bar{q}_i/dt$.

A common approximation is that given by the linear driving force (LDF) model of Glueckauf and Coates [10]

$$\frac{d\bar{q}_i}{dt} = \frac{K_{LDF_i} D_{e_i}^*}{r_p^2}\left(q_i^* - \bar{q}_i\right) \tag{4}$$

For the typical particle size range used in RPSA as in this work, macropore diffusion has been shown to be the dominant transport resistance within the adsorbent particles [3,5,11].

Choong [11] has shown that the values of K_{LDF} for both oxygen and nitrogen could be approximated as 15 for the process conditions used here. The governing equations for the LDF model are:

$$\frac{\partial P}{\partial t} = -\frac{1}{\varepsilon_b}\left\{\frac{\partial (uP)}{\partial z} + \rho_b RT \sum_i \frac{d\overline{q}_i}{dt}\right\} \tag{5}$$

and

$$\frac{\partial y_A}{\partial t} = -\frac{1}{\varepsilon_b P}\left\{\frac{\partial (uPy_A)}{\partial z} - D\frac{\partial}{\partial z}\left(P\frac{\partial y_A}{\partial z}\right) + \rho_b RT\frac{d\overline{q}_A}{dt}\right\} - \frac{y_A}{P}\frac{\partial P}{\partial t} \tag{6}$$

3.3 Initial Conditions

For the first cycle of the transient simulation, the bed is initially filled with ambient air and the adsorbent particles are in equilibrium with the ambient air.

For $t = 0$ and for all z:

$$P = P_{am}; \quad y_A = y_{A,am}; \quad \overline{q}_i = H_i P_{am} y_{i,am} / R_g T_{am} \tag{7}$$

3.4 Boundary Conditions

Pressurisation step

At the feed end of the bed (z = 0), the BCs are:

(1) A step change in the feed gas pressure:

$$P\big|_{z=0} = Pf \tag{8}$$

(2) The mole fraction of oxygen is described by the modified boundary condition at the entrance [4]:

$$D\frac{\partial y_A}{\partial z}\bigg|_{z=0} = u\big|_{z=0}\left(y_A\big|_{z=0} - y_{A,f}\right) \tag{9}$$

At the product end of the bed ($z = L$), the BCs are:

(1) Gas flow at constant delivery rate, $\overline{Q}_p$ ($m^3 s^{-1}$ at ambient conditions) and assuming the flow at the product end is in the viscous flow regime yields:

$$P\frac{dP}{dz}\bigg|_{z=L} = -\frac{\overline{Q}_p J_v T P_{am}}{A T_{am}}\bigg|_{z=L} \tag{10}$$

(2) The mole fraction of oxygen is described by the modified boundary condition for the exit [4]:

$$\frac{\partial y_A}{\partial z}\bigg|_{z=L} = 0 \tag{11}$$

Depressurisation step

At the feed end of the bed (z = 0), the BCs are:

(1) A step change in the exhaust gas pressure:

$$P\big|_{z=0} = P_{am} \tag{12}$$

(2) The mole fraction of oxygen is described by the modified BC for the exit [4]:

$$\frac{\partial y_A}{\partial z}\bigg|_{z=0} = 0 \tag{13}$$

The BCs for the depressurisation step at the product end ($z = L$) are as for those of the pressurisation step as given by Equations (10) and (11).

4.0 NUMERICAL SIMULATION

Two methods of spatial discretisation were considered, such as the methods of OC and OCFE. Detailed information on the method of OC can be found in Villadsen and Michelsen [12] and Rice and Do [13]. A summary of the methods of OC and OCFE can be found in Choong [11]. The use these methods are briefly described below.

The method of OC [12] belongs to a type of discretisation methods known as the method of weighted residuals. Among the many variations of weighted residual methods, the Galerkin method provides the best accuracy. However, the OC method is often the preferred method as its formulation is convenient to apply and program. Furthermore, the accuracy of OC is found to approach that of the Galerkin method [12,13].

In the OC method, the space domain is first transformed into the range [0,1]. The normalised space domain is then divided into $J + 2$ grid points consisting of J interior collocation points, and the two boundary points, $j = 1$ and $j = J + 2$. The interior collocation points are not equally spaced, but chosen to be the roots of the Jacobi

orthogonal polynomial, $P_J^{(\alpha,\beta)}$, where α and β are integers. The variation of α and β has been found to have little effect on the solution [14]. In this study, α and β are chosen as zero, which gives rise to a subset of Jacobi polynomials known as the Legendre polynomials.

The application of the OC method is as follow. The required number of interior collocation points, J, is first decided and the collocation points are calculated to be the roots of the Jacobi orthogonal polynomial of degree J. The PDEs are then discretised into ODEs on the collocation points chosen, with spatial derivatives of the dependent variables replaced with the derivatives of the Langrangian interpolation polynomials.

The OCFE method is a discretisation scheme that combines the method of OC with the finite element method. The concept was first proposed by Paterson and Cresswell [15]. Its full formulation was described by Carey and Finlayson [16]. In the OCFE method, the space domain is divided into a number of elements, and orthogonal collocation is applied to each of these elements. Collocation points can be concentrated in the region where sharp gradients are expected.

At the element boundaries, continuity of the solution and its first derivative is imposed, together with the two BCs, to form a system of algebraic equations, which is solved before every integration step. For the purpose of programming, the algebraic equations are assembled in a global way by introducing a global indexing scheme.

4.1 Computer Programs

Three separate computer programs written in FORTRAN 77 have been developed for the simulation of the RPSA models. These are the OC method for the ILE model, the OC method for the LDF model, and the OCFE method for the ILE model. The OCFE scheme considered in this work is of equal-sized elements with the same number of interior collocation points for each element. The simulation are carried out on a SUN ULTRA Enterprise 2 (170 MHz) workstation. Several standard algorithms from the NAG FORTRAN library (Mark 16) were employed as external subroutines. The ODE integration algorithm employed the NAG FORTRAN library subroutine D02EJF, which is based on a variable order, variable step method implementing backward differentiation formulae, and is suitable for a stiff system of first order non-linear ODEs. The accuracy of the integration is controlled by the absolute tolerance, TOL, used in the subroutine.

In the OCFE, element continuity with pressure as a dependent variable gives rise to a set of non-linear algebraic equations. This set of non-linear algebraic equations is solved using the NAG FORTRAN library subroutine C05NBF, which was based on a modification of the Powell hybrid method. Element continuity with oxygen mole fraction as a dependent variable gives rise to a set of linear algebraic equations, which is solved here using NAG FORTRAN library subroutine F04EAF. This subroutine was based on Gaussian elimination with partial pivoting.

Note that Alpay [3] suggested solving the element continuity calculations using NAG FORTRAN library subroutine F04EAF. This subroutine is suitable for solving only linear algebraic equations, and may not be appropriate for solving algebraic equations that are non-linear as in the case of pressure as a dependent variable. Therefore, the status of his simulation results was unclear.

4.2 Validation of the Discretisation Methods

The OC and OCFE methods are first used to simulate the heat conduction in a finite slab for which analytical equations could be obtained. For OC, a polynomial of order 50 is used. For OCFE, 5 equally sized elements with polynomial of order 10 in each element are used. The equation for linear heat conduction is given as:

$$\frac{\partial T}{\partial t} = \alpha_h \frac{\partial^2 T}{\partial z^2} \tag{14}$$

A slab with thickness $2L = 3.0 \times 10^{-2}$ m, $ah = 5.0 \times 10^{-4}$ m^2 s^{-1} and initial temperature, $T_{init} = 1000$°C is suddenly immersed into an ice bath of 0°C. The temperature profile inside the slab in this case is symmetric.

The BCs are:

$$T\big|_{z=0} = 0; \qquad \left.\frac{\partial T}{\partial z}\right|_{z=L} = 0 \tag{15}$$

The analytical solution is given as [17]:

$$T = \frac{4T_{init}}{\pi} \sum_{n=0}^{\infty} \frac{1}{(2n+1)} exp\left(\frac{-\alpha_h (2n+1)^2 \pi^2 t}{(2L)^2} \right) sin \frac{(2n+1)\pi z}{2L} \tag{16}$$

Figure 2 shows T as a function of the dimensionless length (z/L), calculated using the OC method. The agreement between the simulation results and the analytical solution, Equation (16), is excellent. Similar results were obtained for the OCFE method.

4.3 Validation of RPSA Models

The simulation programs were validated by simplifying the RPSA models to compare the numerical calculations with the similarity solutions obtained by Scott [7]. He produced semi-analytical solutions for the pressurisation and depressurisation of a semi-infinite adsorptive bed which preferentially adsorbs one component of a binary gas mixture, under the following conditions: gas flow in the bed is governed by Darcy's Law, the adsorption process is isothermal and at equilibrium, the isotherms are linear, and there is no axial dispersion. The bed is initially at atmospheric conditions. PDEs

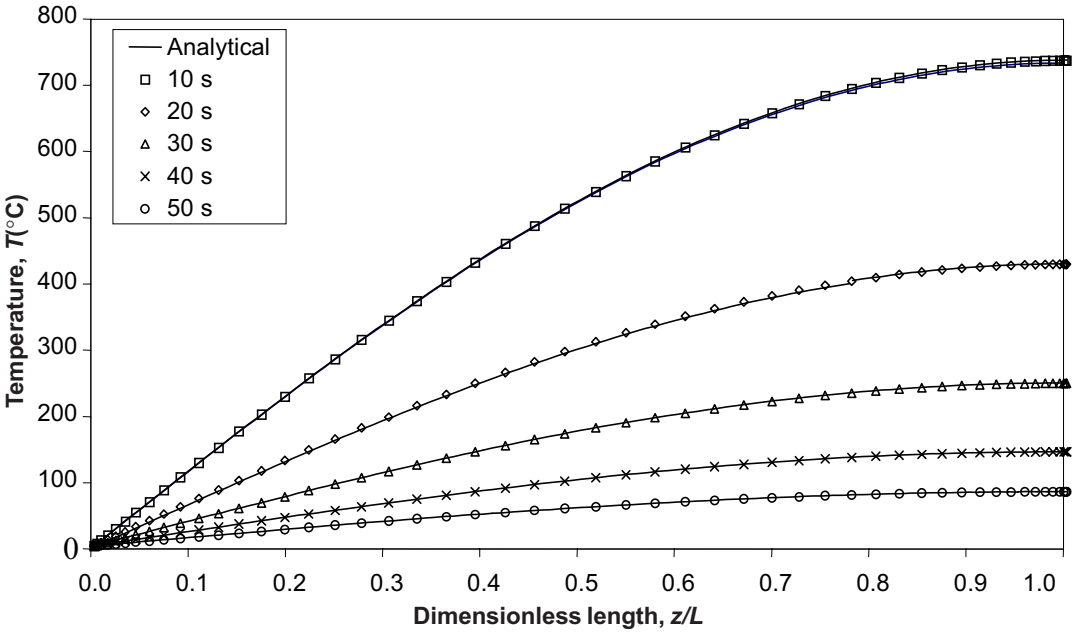

Figure 2 OC: Comparison of the numerical calculations and the analytical solution of heat conduction in a slab of thickness 2L. Similar results were obtained using the method of OCFE

obtained for each gas component were reduced to ODEs by introducing a similarity variable, η, defined as:

$$\eta = \left(\frac{J_v}{tP_{am}} \right)^{1/2} L_{ref} \tag{17}$$

A packed bed consists of spherical zeolite 5Å particles, with bed porosity, $\varepsilon_b = 0.4$, is used. Air at 2.0 bar with 21% oxygen and 79% nitrogen is taken to be the feed. Taking bed bulk density, ρ_b, as 800 kg m^{-3}, Henry's law constants for oxygen and nitrogen are given as 6.11×10^{-3} m^3/kg and 2.0×10^{-2} m^3/kg, respectively. The reference bed length, L_{ref}, is taken as 8.0 m to represent a semi-infinite bed. A constant value of the effective axial dispersion coefficient, $D = 1.0 \times 10^{-5}$ m^2/s is used in the numerical model to approach the plug flow condition.

Figures 3 and 4, show graphs of oxygen mole fraction and total bed pressure profile at different times after pressurisation, simulated by the OC and OCFE, respectively as a function of the similarity variable, η. The agreement between the simulated total bed pressure profiles and the similarity solutions is excellent. The shape of the simulated oxygen mole fraction profiles and the position of the shocks are in good agreement with the similarity solutions obtained by Scott [7]. However, numerical oscillations before and after the shocks are observed. A large number of grid points may be required to track the shocks accurately. For OCFE, the shocks are not captured as well

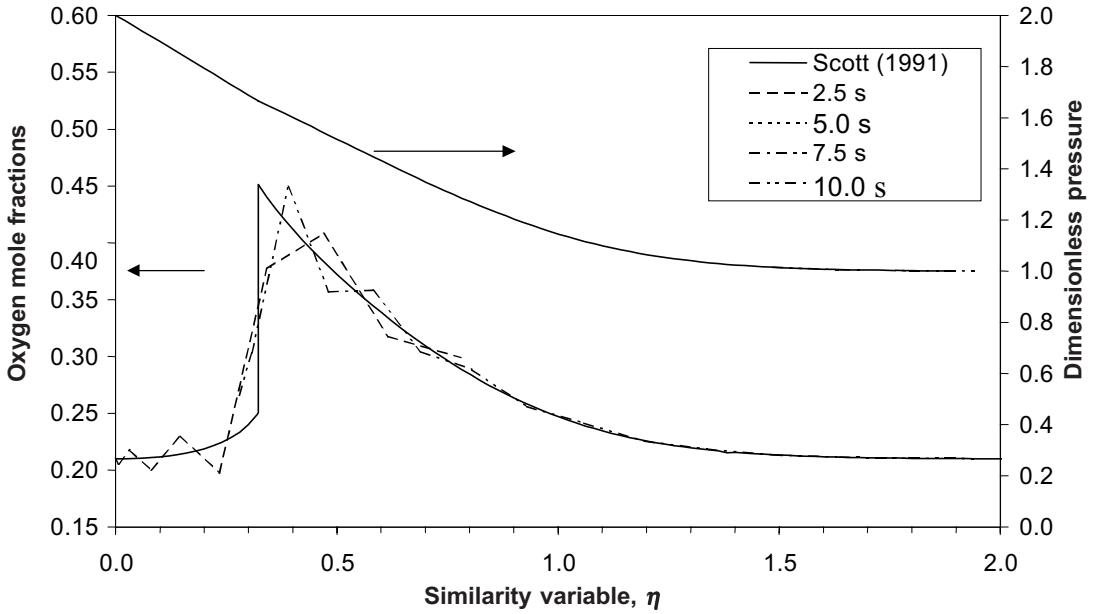

Figure 3 OC/ILE: Comparison of the numerical calculations and the similarity solutions for pressurisation. Simulated dimensionless pressure overlaps with the similarity solutions of Scott [7]

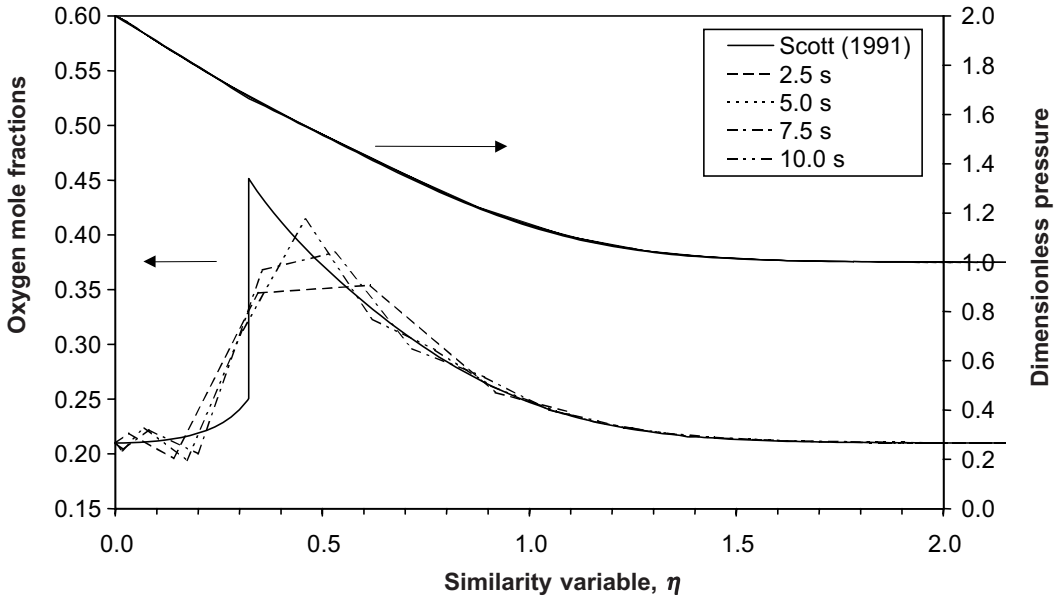

Figure 4 OCFE/ILE: Comparison of the numerical calculations the similarity solutions for pressurisation. The method of OCFE using 5 equally sized elements with polynomial of order 10 in each element was used. Simulated dimensionless pressure overlaps with the similarity solutions of Scott [7]

as they were by OC. Improved agreement between the simulations of OCFE and the semi-analytical solution can be achieved by concentrating collocation points in the element where a sharp gradient is expected.

The numerical oscillations observed before and after the shocks could be reduced by introducing a large constant value of axial dispersion, such as $D = 1.0 \times 10^{-2}$ m^2/s. However, the maxima of the oxygen mole fraction peaks are significantly reduced [11]. While the effective axial dispersion coefficient has a profound effect on oxygen mole fraction, it has no effect at all on the total pressure, as the model does not imply axial dispersion of total material [4]. As for depressurisation, the agreement between the numerical calculations and the similarity solutions is excellent, as shown in Figure 5. This indicates that the modified BCs used to describe the BCs at the feed end during pressurisation are satisfactory.

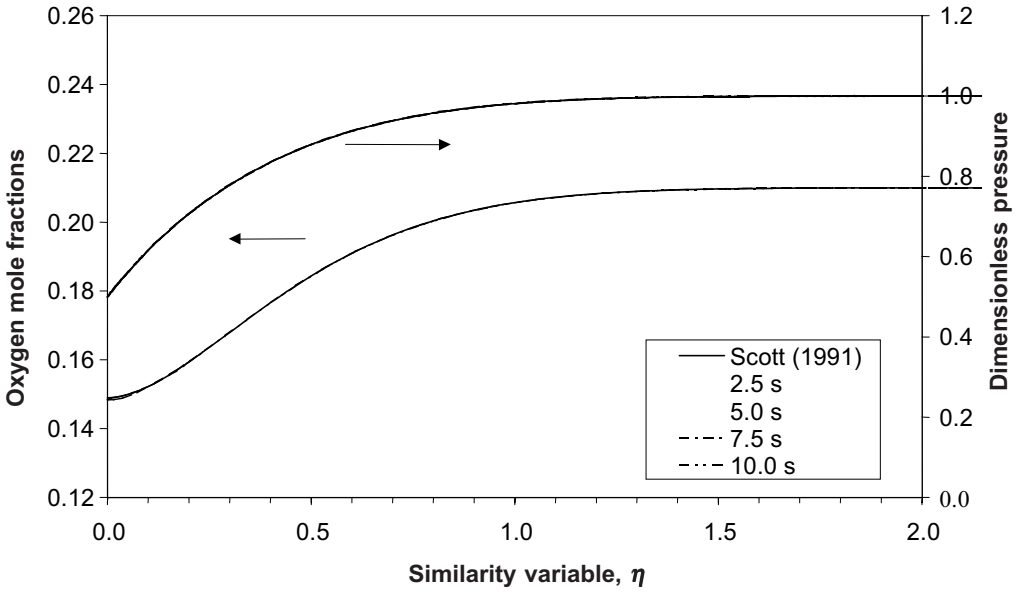

Figure 5 Comparison of the numerical calculations and the similarity solutions for depressurisation. Simulated dimensionless pressure and oxygen mole fraction overlap with the similarity solutions of Scott [7] for all three cases considered in this work

Simulation results on the validation of the LDF model are not reported here. These were described in detail in Choong [11].

4.4 Conservation of Mass in RPSA

Because of discretisation error and rounding error, our numerical simulations will not perfectly conserve mass. The conservation error is computed as a guide to the numerical

accuracy of our calculations. The component balance relative error, Err_i, for one step is defined as:

$$Err_i = \left| \frac{M_{i,feed} - M_{i,accum} - M_{i,product}}{M_{i,feed}} \right| \times 100\% \tag{18}$$

where the subscript i refers to component A or component B, and

$$M_{i,feed} = A \int_0^{t'} (ucy_i)_f \, dt \tag{19}$$

and

$$M_{i,product} = A \int_0^{t'} (ucy_i)_{z=L} \, dt \tag{20}$$

where t' is any time measured from the start of a step.

For an ILE model

$$M_{i,accum} = A \left\{ \int_0^L \left[(\varepsilon_i c y_i + \rho_b q_i^*) - (\varepsilon_i c y_i + \rho_b q_i^*)_{init} \right] dz \right\} \tag{21}$$

and for an LDF model

$$M_{i,accum} = A \left\{ \int_0^L \left[(\varepsilon_b c y_i + \rho_b \bar{q}_i) - (\varepsilon_b c y_i + \rho_b \bar{q}_i)_{init} \right] dz \right\} \tag{22}$$

The space integrals in Equations (21) and (22) are evaluated using the NAG subroutine D01GAF, which employs a third order finite difference method. The number of collocation points in the space domain determines the number of quadrature points in the space integrals. Therefore, no additional adjustable parameter is introduced.

Because the velocity changes rapidly with time at the feed end of the bed, the application of quadrature using the NAG subroutine D01GAF as adopted by Alpay [3] to evaluate the time integral does not provide the accuracy required. This difficulty can be overcomed by transforming all the equations involving time integrals into ODEs. After the transformation, the accuracy of the time integral is maintained by the ODE solver. This transformation not only allows us to calculate accurately the time integrals, it also minimises the number of decision parameters that need to be specified for the computer program. The superiority of the transformation over quadrature has been demonstrated convincingly by considering a simple problem of pressurisation and depressurisation of air into a non-adsorptive packed bed.

5.0 ACCURACY AND CPU TIME ANALYSIS

The accuracy of the numerical solutions now depends on only two parameters, such as the number of interior collocation points in the space domain and the value of the

absolute tolerance, TOL, used in the ODE integration algorithm. For the method of OC, the number of interior collocation points equals the order of polynomial chosen. For OCFE, the number of interior collocation points depends on the number of elements and the order of polynomial used in each element (excluding the element-element boundaries). Since there are many possible combinations of spatial discretisations in OCFE, only OCFE of 5 equally sized elements, with polynomials of the same order in each element, is considered. Both Alpay [3] and Murray [5] used OCFE of 5 equally sized elements in their simulations. However, the decision to use 5 equally sized elements in OCFE in this work is arbitrary. The effect of varying the number of interior collocation points and the value of TOL are next investigated.

For the purpose of this analysis, the process conditions listed in Table 1 were used for all simulations. The NAG FORTRAN library subroutine DO2EJF with absolute tolerance, TOL = 1×10^{-5}, was used for the integration of the system of ODEs. Since oxygen product purity is an important design parameter in RPSA, it was used in this study as the key parameter for measuring the accuracy of simulations. The CPU time

Table 1 Operating conditions for RPSA simulations

Operating variable	Description	Unit	Value
d_c	bed diameter	m	0.05
L	bed length	m	1.0
P_f	feed pressure	bar	1.84
T	temperature	K	290
ε_b	bed porosity		0.35
ε_p	particle porosity		0.55
ρ_b	bed bulk density	kg m^{-3}	800
H_A	Henry's law constant for oxygen	m^3 kg^{-1}	3.5×10^{-3}
H_B	Henry's law constant for nitrogen	m^3 kg^{-1}	7.7×10^{-3}
t_c	cycle time	s	3.0
d_p	particle diameter	m	2.0×10^{-4}
D	effective axial dispersion coefficient	m^2 s^{-1}	1.0×10^{-3}
$\bar{Q}_p$	product delivery rate	m^3 s^{-1} @ P_{am}, T_{am}	1.0×10^{-5}
$D^*_{eO_2}$	modified effective disffussion coefficient for O_2	m^2 s^{-1}	2.66×10^{-7}
$D^*_{eN_2}$	modified effective disffussion coefficientfor N_2	m^2 s^{-1}	1.24×10^{-7}

is measured in terms of seconds per cycle at CSS. The CSS is calculated using the method of successive substitution (MSS). The simulation involves a series of complete cycles with the results of the previous cycle used as initial conditions for the next cycle. It is first assumed that CSS is reached after 2000 cycles of pressurisation and depressurisation. The CSS is later confirmed using the rational stopping criterion developed by Choong *et al.* [18].

5.1 Variation of the Number of Interior Collocation Points

The use of a small number of interior collocation points gives a low accuracy while a large number of interior collocation points give a high accuracy. However, the number of ODEs generated increases linearly with the number of interior collocation points, resulting in an increase in computational time for solutions. For practical simulation, a compromise has to be made between accuracy and CPU times.

The OC and OCFE methods were compared for an ILE model. Simulation results with different number of interior collocation points using the OC and OCFE methods are given in Tables 2 and 3, respectively. The OC and OCFE give identical oxygen product purity at CSS, $y_p^{(\infty)}$, to four significant figures (s.f.) with very similar CPU times for the largest number of interior collocation points used in this study, such as 50 interior collocation points. The absolute differences between the calculated oxygen product purity at CSS and that of the 50 interior collocation points, measured in terms of absolute percentage points are shown to diminish rapidly as the number of interior collocation points approached 20, but thereafter more slowly as the number of interior collocation points increased. The OC method is found to give comparable accuracy to the OCFE method for 20 and 30 interior collocation points, albeit requiring more computing time. However, it is not our intention to optimise the spatial discretisation.

Table 2 OC/ILE: Effect of total number of interior collocation points (J) on the accuracy of oxygen product purity and CPU time at CSS. Process conditions are listed in Table 1. TOL used is 1×10^{-5}. Δ is the absolute difference between $y_p^{(\infty)}$ of J and $y_p^{(\infty)}$ of $J = 50$.

J	$y_p^{(\infty)}$ (%)	Δ (%)	CPU time (s cycle^{-1})	Err_i (%) for 1st cycle, Eq. (23)			
				Pressurisation		Depressurisation	
				Oxygen	Nitrogen	Oxygen	Nitrogen
5	49.87	18.54	0.22	0.4610	1.5700	1.5200	2.3500
10	70.41	2.00	0.45	0.4320	0.1430	0.0099	0.5230
20	68.84	0.43	2.70	0.0443	0.0286	0.0356	0.0564
30	68.53	0.12	8.25	0.0098	0.0098	0.0187	0.0154
50	68.41	0.00	42.65	0.0027	0.0023	0.0052	0.0033

Table 3 OCFE/ILE: Effect of total number of interior collocation points (J) on the accuracy of oxygen product purity and CPU time at CSS. Process conditions are listed in Table 1. TOL used is 1×10^{-5}. Five equally sized elements with the same order of polynomial (J') in each element are used. Δ is the absolute difference between $y_p^{(\infty)}$ of J and $y_p^{(\infty)}$ of $J = 50$.

J'	J	$y_p^{(\infty)}$ (%)	Δ (%)	CPU time (s cycle^{-1})	Err_i (%) for 1st cycle, Eq. (23)			
					Pressurisation		Depressurisation	
					Oxygen	Nitrogen	Oxygen	Nitrogen
1	5	44.50	23.90	0.210	2.84	4.6300	12.800	24.500
2	10	56.70	7.70	0.534	0.282	2.2200	0.886	4.4500
4	20	68.50	0.10	1.730	0.343	0.4800	0.979	0.7490
6	30	68.50	0.10	4.300	0.148	0.1900	0.417	0.2510
10	50	68.40	0.00	43.80	0.0546	0.0445	0.100	0.0677

The method of OC is considered sufficient for the development of novel algorithm features for processes that exhibit CSS.

Table 4 shows the oxygen product purity at CSS for different interior collocation points, for an LDF model simulated using the OC method. A trend similar to that of an ILE model is observed, such as the oxygen product purity at CSS is found to steady out after 20 interior collocation points. As expected, due to the additional ODEs arising from the adsorption rate equations, the LDF model requires much more computing time compared to an ILE model, as given in Table 2.

Table 4 OC/ILE: Effect of total number of interior collocation points (J) on the accuracy of oxygen product purity and CPU time at CSS. Process conditions are listed in Table 1. TOL used is 1×10^{-5}. Δ is the absolute difference between $y_p^{(\infty)}$ of J and $y_p^{(\infty)}$ of $J = 50$.

J	$y_p^{(\infty)}$ (%)	Δ (%)	CPU time (s cycle^{-1})	Err_i (%) for 1st cycle, Eq. (23)			
				Pressurisation		Depressurisation	
				Oxygen	Nitrogen	Oxygen	Nitrogen
5	50.91	15.13	0.56	0.0782	1.3230	1.2640	1.8020
10	66.30	0.26	2.30	0.2540	0.0543	0.2020	0.2800
20	65.97	0.07	9.65	0.0013	0.0024	0.0015	0.0066
30	66.04	0.00	25.31	0.0005	0.0006	0.0013	0.0012
50	66.04	0.00	121.10	0.0001	0.0002	0.0001	0.0003

From simulation results reported in Tables 2 to 4, it is found that the number of interior collocation points has a rather profound effect on the CPU time. For example, for an ILE model simulated using the OC method as reported in Table 2, the CPU time required for 50 interior collocation points is about a factor of 20 greater than that for 20 interior collocation points, and a factor of 100 greater than that for 10 interior collocation points. However, the accuracy of oxygen product purity at CSS calculated using 10 interior collocation points is within two percentage points of that of the 50 interior collocation points.

5.2 Variation of TOL in the ODE Integration Algorithm

The effect of TOL on $y_p^{(\infty)}$ and CPU time at CSS is studied using the method of OC for both ILE and LDF models. A reduction in TOL usually leads to an approximately proportional reduction error in the solution. However, a smaller tolerance requires smaller integration time steps in order to maintain the accuracy required. Subsequently, more computing time is required for the integration. The oxygen product purity at CSS steadies out after TOL = 1×10^{-4}. The effect of TOL is found to have a less profound effect on the CPU time. Decreasing TOL by an order of magnitude increases the CPU time by about 10%. From Tables 5 and 6, which show the effect of TOL on $y_p^{(\infty)}$ and CPU time for the ILE and LDF models, respectively, it is decided that TOL = 1×10^{-5} is sufficient for the simulations in this work. As a rule of thumb, the value of the tolerance used in the ODE solver might be estimated from

$$\text{TOL} = 10^{-(acc+1)} \tag{23}$$

where *acc* is the number of significant figures specified in the product purity.

Table 5 OC/ILE: Effect of total number of interior collocation points (J) on the accuracy of oxygen product purity and CPU time at CSS. Process conditions are listed in Table 1. TOL used is 1×10^{-5}. Δ is the absolute difference between $y_p^{(\infty)}$ of J and $y_p^{(\infty)}$ of $J = 50$.

J	$y_p^{(\infty)}$ (%)	Δ (%)	CPU time (s cycle^{-1})	Err_i (%) for 1st cycle, Eq. (23)			
				Pressurisation		Depressurisation	
				Oxygen	Nitrogen	Oxygen	Nitrogen
1×10^{-1}	49.40	19.44	1.50	1.9250	0.9500	1.0330	0.3330
1×10^{-2}	68.82	0.02	1.70	0.1560	0.1500	0.1790	0.0039
1×10^{-3}	68.93	0.09	2.10	0.0638	0.0198	0.0733	0.0415
1×10^{-4}	68.84	0.00	2.47	0.0422	0.0300	0.0316	0.0581
1×10^{-5}	68.84	0.00	2.70	0.0443	0.0286	0.0356	0.0564

Table 6 OC/LDF: Effect of TOL on the accuracy of oxygen product purity and CPU time at CSS. Process conditions are listed in Table 1. The order of polynomial used is 20. Δ is the absolute difference between $y_p^{(\infty)}$ of TOL and $y_p^{(\infty)}$ of TOL = 1×10^{-5}.

TOL	$y_p^{(\infty)}$ (%)	Δ (%)	CPU time (s cycle^{-1})	*Err*$_i$ (%) for 1st cycle, Eq. (23)			
				Pressurisation		Depressurisation	
				Oxygen	Nitrogen	Oxygen	Nitrogen
1×10^{-1}	50.91	15.06	0.55	2.4600	0.6550	0.6680	0.1320
1×10^{-2}	67.03	1.06	6.29	0.0760	0.0222	0.1670	0.0411
1×10^{-3}	65.88	0.09	8.49	0.0090	0.0044	0.0108	0.0091
1×10^{-4}	65.98	0.01	9.03	0.0007	0.0023	0.0004	0.0070
1×10^{-5}	65.97	0.00	9.65	0.0013	0.0024	0.0015	0.0066

5.3 Conservation Error as a Guide to the Spatial Discretisation and TOL

The numerical analysis performed was tedious and time-consuming as about 2000 cycles of pressurisation and depressurisation were required to reach CSS. Therefore, we decided to use the conservation errors at the end of the first pressurisation step and depressurisation step for screening the combination of spatial discretisation and TOL before performing a more rigorous numerical analysis. This might be particularly useful for OCFE where a large possible set of combinations of number of elements, order of polynomials and TOL exists. The conservation errors at the end of the first pressurisation step and depressurisation step are reported in Tables 2 to 6. Observe that reasonable accuracy of oxygen product purity at CSS can be achieved provided that the component material balance relative error for each individual step at the first cycle is within 1 %. However, it should be noted that the values of the relative component material balances errors change with the number of cycles (either increasing or decreasing) and no consistent trend could be found in the numerical analysis performed here.

6.0 DISCUSSION

In a similar study using the process conditions listed in Table 1, Alpay *et al.* [18] reported that the component material balance relative errors for each individual step at CSS was met to within 10 % using the OCFE method with 5 equally sized elements with polynomial of order 4 in each element. The time integrals for molar flowrates into and out of the bed were evaluated by Alpay *et al.* [19] using NAG subroutine D01GAF with 50 equally spaced time points. Using a similar OCFE scheme, the component material balance relative errors for each individual step at CSS obtained in this work

was within 2 %. The improved material balance closure that we obtained could be attributed to the use of a physically consistent model formulation and a more accurate method for evaluating the time integrals for molar flowrates into the bed.

Nilchan [6] gave an alternative form of calculating the conservation of mass for cyclic process. At CSS, the conditions at the end of each cycle were identical to those at its start in both gas and solid phases. Therefore, over a complete cycle, the cumulative molar amount of component i fed to the bed, $M_{i,f}^{(\infty)}$, must, in principle, equal the sum of the cumulative molar amount of component i collected in the product stream, $M_{i,product}^{(\infty)}$ and the cumulative molar amount of component i collected in the exhaust stream, $M_{i,e}^{(\infty)}$. The relative component balance error at CSS, $Err_i^{(\infty)}$, is given as:

$$Err_i^{(\infty)} = \left| \frac{M_{i,f}^{(\infty)} - M_{i,product}^{(\infty)} - M_{i,e}^{(\infty)}}{M_{i,f}^{(\infty)}} \right| \times 100\% \tag{24}$$

where the superscript (∞) refers to conditions at CSS. Equation (16) is restricted only to the condition at CSS, and thus it is of limited use in monitoring the discretisation error and rounding error of numerical simulations.

7.0 CONCLUSION

Both physically consistent RPSA models are solved numerically by spatially discretisating the governing PDEs to a system of ODEs, which are then integrated over time using an ODE integration algorithm, NAG FORTRAN library subroutine DO2EJF. Two spatial discretisation methods are considered, namely the methods of OC and OCFE. Both the OC and OCFE codes are first validated by comparing the numerical solutions with the analytical solutions of of heat conduction in a finite slab. Excellent agreement between the simulations and analytical solutions is obtained for both OC and OCFE methods. The RPSA simulation programs are then validated by simplifying the process models to compare the numerical results with similarity solutions obtained by Scott [17] for air pressurisation and depressurisation into a semi-infinite adsorbing bed. For pressurisation, the predicted oxygen mole fraction profiles and the position of the shock are in good agreement with the similarity solution for both OC and OCFE. However, numerical oscillations are observed before and after the predicted shock. As for depressurisation, the agreement between the numerical results and the similarity solution is excellent for both OC and OCFE.

The error in conservation of mass is computed as a guide to the numerical accuracy of the calculations. To obtain good accuracy, all the equations involving time integrals are transformed into ODEs. This transformation also minimises the number of decision parameters that need to be specified for the computer program. With the transformation, the accuracy of the numerical calculations depends only on the spatial discretisation and the tolerance used in the ODE integration algorithm.

This paper concluded with a study on the effect of the number of collocation points and tolerance used in the ODE integration algorithm on the accuracy of the numerical solutions and the CPU time required. The method of OC is found to give accuracy comparable to that of the method of OCFE, albeit requiring more computing time. However, optimisation of spatial discretisation is not attempted here. We consider the method of OC sufficient for the purpose of our work, such as to design an algorithm for modelling processes that exhibit CSS. In our subsequent work, all simulations are performed using the OC method with a 20^{th} degree polynomial. The TOL used in the ODE integration can be estimated using the rule of thumb given in Equation (23).

REFERENCES

[1] Ruthven, D.M., S. Farooq and K.S. Knaebel. 1994. *Pressure Swing Adsorption*. New York: VCH Publishers.
[2] Hassan, M.M., N.S. Raghavan and D.M. Ruthven.1987. Numerical Simulation of a Pressure Swing Air Separation System - a Comparative Study of Finite Difference and Collocation Methods. *Can. J. Chem. Eng.* 65: 512–515.
[3] Alpay, E. 1992. *Rapid Pressure Swing Adsorption Processes.* Ph.D. Thesis, University of Cambridge.
[4] Choong, T.S.Y., D.M. Scott and W.R. Paterson. 1998. Axial Dispersion in Rich, Binary Gas Mixtures: Model Form and Boundary Conditions. *Chemical Engineering Science*. 53: 4147–4149.
[5] Murray, J.W. 1996. *Air Separation by Rapid Pressure Swing Adsorption*. Ph.D. Thesis, University of Cambridge.
[6] Nilchan, S. 1997. *The Optimisation of Periodic Adsorption Processes*. Ph.D. Thesis, University of London.
[7] Scott, D.M. 1991. Similarity Solutions for Pressurisation and Depressurisation with a Two-component Gas in an Adsorbing Bed. *Chem. Engng Sci.* 46: 2977–2982.
[8] Turnock, P.H. and R.H. Kadlec. 1971. Separation of Nitrogen and Methane via Periodic Adsorption. *A.I.Ch.E. J.* 17: 335–342.
[9] Macdonald, I. E., M.S. El-Sayed, K. Mow and F.A.L. Dullien. 1979. Flow through Porous Media - the Ergun Equation Revisited. *Ind. Engng. Chem. Fundam*. 18: 199–207.
[10] Glueckauf, E. and J.I. Coates. 1947. Theory of Chromatography. Part IV. The Influence of incomplete Equilibrium on the Front Boundary of Chromatograms and on the Effectiveness of Separation. *J. Chem. Soc.* 1315–1321.
[11] Choong, T.S.Y. 2000. *Algorithm Synthesis for Modelling Cyclic Processes: Rapid Pressure Swing Adsorption*. Ph.D. Dissertation, University of Cambridge.
[12] Villadsen, J.V. and M.L. Michelson. 1978. *Solution of Differential Equations by Polynomial Approximation*. New Jersey: Prentice-Hill.
[13] Rice, R.G. and D.D. Do. 1995. *Applied Mathematics and Modelling for Chemical Engineers*. John Wiley & Sons, U.S.A.
[14] Liow, J.L. 1986. *Air Separation by Pressure Swing Adsorption*. Ph.D. dissertation, University of Cambridge.
[15] Paterson, W.R. and D.L. Creswell. 1971. A Simple Method for the Calculation of Effectiveness Factors. *Chem. Engng Sci.* **26**: 605–616.
[16] Carey, G. F. and B. A. Finlayson. 1975. Orthogonal Collocation on Finite Elements. *Chem. Eng. Sci.* 30: 587–596.
[17] Carslaw, H. S. and J. C. Jaeger. 1986. *Conduction of Heat in Solids*. 2nd Edition. Oxford: Clarendon Press.
[18] Choong, T.S.Y., D.M. Scott and W.R. Paterson. 2002. Development of Novel Algorithm Features in the Modelling of Cyclic Processes. *Computers Chem. Eng.* 26: 95–112.
[19] Alpay, E., C. N. Kenney and D. M. Scott. 1993. Simulation of Rapid Pressure Swing Adsorption and Reaction Processes. *Chem. Eng. Sci.* 48: 3173–318.

NOTATION

A	bed cross sectional area	m^2
c	gas phase concentration	mol m^{-3}
dc	bed diameter	m
dp	particle diameter	m
D	effective axial dispersion coefficient	m^2 s^{-1}
Err	relative material balance error	%
i	an index	
j	an index	
J	order of polynomial in the method of OC	
H	Henry's law constant	m^3 kg^{-1}
L	length of bed	m
M	cumulative molar amount at any time during a step	
N	number of space discretisation points	
P	total bed pressure	Pa
	product delivery rate	m^3 s^{-1}
	ideal gas constant	J mol^{-1} K^{-1}
u	superficial gas velocity	m s^{-1}
t	time	s
t'	any time measured from the start of a step	s
t_c	cycle time	s
T	temperature	K or °C
y	gas phase mole fraction	
y_p	oxygen product purity averaged over a complete cycle	
z	axial co-ordinate	m

Greek letters

α, β	integers in Jacobi orthogonal polynomials	
α_h	thermal diffusivity	m^2 s^{-1}
Δ	absolute difference between two values	
ε_b	bed porosity	
ε_p	particle porosity	
η	similarity variable defined by Equation (22)	
ρ_b	bed bulk density	kg m^{-3}

Subscripts

am	ambient conditions
accum	accumulation in the bed
A, B	component A (oxygen) or component B (nitrogen)

e	exhaust conditions
f	feed, far upstream of $z = 0$
feed	feed end of the bed
i	component *i*
init	initial values
product	product end of the bed

Superscripts

acc	significant figures specified in the product purity
(∞)	at CSS

Abbreviations

CPU	computer processing unit
CSS	cyclic steady state
gPROMS	general PROcess Modelling System
ILE	instantaneous local equilibrium
LDF	linear driving force
MSS	method of successive substitution
OC	orthogonal collocation
OCFE	orthogonal collocation on finite element
ODE	ordinary differential equation
PDE	partial differential equation
RPSA	rapid pressure swing adsorption
TOL	tolerance used in the ODE solver